

ARMY RESEARCH LABORATORY



# Steady-State Potential Scan at Rotating Disk Electrode and Applications

Rongzhong Jiang, Charles Walker, and Deryn Chu

ARL-TR-2230

August 2000

Approved for public release; distribution unlimited.

DTIC QUALITY INSPECTED 4

20000925 075

The findings in this report are not to be construed as an official Department of the Army position unless so designated by other authorized documents.

Citation of manufacturer's or trade names does not constitute an official endorsement or approval of the use thereof.

Destroy this report when it is no longer needed. Do not return it to the originator.

# Army Research Laboratory

Adelphi, MD 20783-1197

---

ARL-TR-2230

August 2000

---

## Steady-State Potential Scan at Rotating Disk Electrode and Applications

Rongzhong Jiang, Charles Walker, and Deryn Chu

Sensors and Electron Devices Directorate

---

## Abstract

---

A method of multiple small potential steps was applied to obtain current-potential curves at a rotating disk electrode (RDE), which is more accurate than the classical potential scan RDE method. Several basic benefits of the new RDE method were summarized, including reducing charging current, removing adsorption current, identifying kinetic current, and separating kinetic and diffusion reactions. The practical application of this new method is to study high-surface-area powder catalysts for fuel cell research. An example of using this new method was demonstrated by measurement of the current-potential curves of catalytic oxygen reduction on a heat-treated, metalloporphyrins-coated graphite RDE. A successful kinetic analysis of catalytic oxygen reduction at the powder-catalyst-coated electrode was achieved.

## Contents

<b>1. Introduction .....</b>	<b>1</b>
<b>2. Experimental Setup .....</b>	<b>2</b>
2.1 <i>Materials .....</i>	2
2.2 <i>Apparatus and Procedures .....</i>	2
<b>3. Method .....</b>	<b>3</b>
<b>4. Results and Discussions .....</b>	<b>5</b>
4.1 <i>Reduce Charging Current .....</i>	5
4.2 <i>Remove Adsorption or Electrode Self-Reaction Current .....</i>	6
4.3 <i>Identify Kinetic Current of Species in Bulk Solution .....</i>	6
4.4 <i>Separate Kinetic and Diffusion Reactions .....</i>	7
4.5 <i>An Example of Application .....</i>	8
<b>5. Conclusions .....</b>	<b>10</b>
<b>Acknowledgments .....</b>	<b>10</b>
<b>References .....</b>	<b>11</b>
<b>Distribution .....</b>	<b>13</b>
<b>Report Documentation Page .....</b>	<b>15</b>

## Figures

1. Schematic profiles of multiple small potential steps and resulting current signals at rotating disk electrode .....	4
2. Polarization curves for oxygen reduction at HT-FeTPP-coated RDE in O <sub>2</sub> -saturated 0.5-M H <sub>2</sub> SO <sub>4</sub> solution .....	5
3. Polarization curves for oxygen reduction at Pd-black-coated RDE in O <sub>2</sub> -saturated 0.5-M H <sub>2</sub> SO <sub>4</sub> solution .....	6
4. Polarization curves for methanol oxidation at Pt-black-coated RDE in argon-saturated 0.5-M H <sub>2</sub> SO <sub>4</sub> containing 1.0 M of methanol .....	7
5. Polarization curves for oxygen reduction and methanol oxidation at Pt-black-coated RDE in O <sub>2</sub> -saturated 0.5-M H <sub>2</sub> SO <sub>4</sub> containing 1.0 M of methanol .....	8
6. Polarization curves at various rotation rates for oxygen reduction at HT-FeTPP/CoTPP-coated RDE in O <sub>2</sub> -saturated 0.5-M H <sub>2</sub> SO <sub>4</sub> solution .....	9
7. Koutecky-Levich plot for oxygen reduction at HT-FeTPP/CoTPP-coated RDE in O <sub>2</sub> -saturated 0.5-M H <sub>2</sub> SO <sub>4</sub> solution .....	9

## Table

1. Kinetic rate constants for catalytic oxygen reduction at HT-FeTPP-CoTPP/PG electrode in O <sub>2</sub> -saturated 0.5-M H <sub>2</sub> SO <sub>4</sub> solution .....	9
--	---

# 1. Introduction

The rotating disk electrode (RDE) method [1–2] has been widely used as a powerful tool for studying electrode kinetics. For example, many electrochemical laboratories have used the RDE method to study the kinetics of catalytic oxygen reduction [3–8], which has been recognized as one of the most complex electrode processes. The kinetic rate constants of catalytic oxygen reduction can be easily obtained through a Koutecky-Levich plot [2]. The RDE method requires that the electrode is in a steady state and that the solution has a laminar flow at the electrode surface. This requirement has only been applied to the study of powder catalysts, because powder catalysts may exhibit large charging currents or a turbulent flow of the electrolyte because of their large surface area. In addition, identification of catalytic current from unavoidable adsorption and electrode-self-reaction current is difficult, which causes the current-potential curve by RDE to measure less accurately. An effort has been made to improve the accuracy of the RDE method by linear rotation scan [9]; unfortunately, this measures the current only at a specific potential, and the current-potential curve is not available.

Fuel cells have been considered one of the most promising candidates for innovative energy sources [10–15] for cleaner air and less pollution. The demand for developing room-temperature fuel cells, such as polymer electrolyte membrane fuel cells (PEMFCs), has sped up the research on electrode catalysts. However, practical catalysts, such as fine powders, are used in PEMFCs. To characterize such powder catalysts with an RDE method seems difficult because of their large surface area.

Electrode catalysts are a key electrode component for PEMFCs. To develop a high-power PEMFC, we have tried to use the RDE method to study a series of powder catalysts. Ni and Anson [16] studied a relation between the reduction potentials of adsorbed and unadsorbed  $\text{CoTMP}_y\text{P}$ , by using a zero-scan method to remove the surface response. Based on their work, we introduce an RDE method that uses multiple small potential steps, which can be used to study the electrode kinetics of powder catalysts for PEMFC applications.

## 2. Experimental Setup

### 2.1 Materials

Palladium and platinum powder catalysts were electrochemically pure grade and used as received. Iron (III) tetraphenylporphyrin and cobalt tetraphenylporphyrin (from Aldrich) were heat-treated under argon atmosphere at 600 to 700 °C and ground to fine powder to be used as catalysts.

### 2.2 Apparatus and Procedures

We performed the RDE experiments with a conventional glass cell that had three separate compartments for working, counter, and reference electrodes. A reversible hydrogen electrode (RHE) was used for the reference electrode, and a platinum screen was used for the counter electrode. An ordinary pyrolytic graphite (PG) RDE (0.2 cm<sup>2</sup>) was used for the working electrode. A paste of catalyst with 3 percent Teflon binder was spread on the electrode and dried slowly. For convenience, we called the powder-catalyst-coated RDE electrodes Pd/PG, Pt/PG, HT-FeTPP/PG, and HT-FeTPP/CoTPP/PG, respectively. In this report, HT-FeTPP means heat-treated iron tetraphenylporphyrin, while HT-FeTPP/CoTPP represents a heat-treated catalyst mixture of 50 percent FeTPP and 50 percent CoTPP. Electrolytes (0.5 M H<sub>2</sub>SO<sub>4</sub>) were prepared with distilled water and high-purity sulfuric acid. High-purity argon and oxygen were used for deaeration of the solution.

An EG & G PAR 173 Potentiostat and a 175 Universal Programmer were used for the electrochemical measurements.

### 3. Method

When using the RDE method to study electrocatalysis, we often used the Levich equation and Koutecky-Levich equations:

$$i_L = 0.620 n F A D_o^{2/3} \omega^{1/2} \nu^{-1/6} C_o^* \quad (1)$$

$$i_k = n F A K \Gamma_{\text{cat}} C_o^* \quad (2)$$

$$i^{-1} = i_k^{-1} + i_L^{-1} \quad (3)$$

$$i^{-1} = 1/(n F A K \Gamma_{\text{cat}} C_o^*) + 1/(0.620 n F A D_o^{2/3} \nu^{-1/6} C_o^* \omega^{1/2}) . \quad (4)$$

Here,  $i_L$  (A) is the Levich current for the electrode reaction of a reactive species by a diffusion-controlled process,  $i_k$  (A) is the kinetic current for the reaction of a reactive species at the electrode surface,  $n$  ( $\text{mol}^{-1}$ ) is the electron transfer number per mole of a reactive species,  $F$  ( $\text{A} \cdot \text{s}$ ) is the Faraday constant,  $A$  ( $\text{cm}^2$ ) is the electrode area,  $K$  ( $\text{M}^{-1} \cdot \text{s}^{-1}$ ) is the kinetic rate constant for catalytic reaction,  $\Gamma_{\text{cat}}$  ( $\text{mol}/\text{cm}^2$ ) is the quantity of catalysts on the surface of the electrode,  $C_o^*$  ( $\text{mol}/\text{cm}^3$ ) is the bulk concentration of the reactive species,  $D_o$  ( $\text{cm}^2 \cdot \text{s}^{-1}$ ) is the diffusion coefficient of the reactive species,  $\nu$  ( $\text{cm}^2 \cdot \text{s}^{-1}$ ) is viscosity of water ( $0.01 \text{ cm}^2 \cdot \text{s}^{-1}$ ), and  $\omega$  ( $\text{s}^{-1}$ ) is the rotation rate ( $2\pi f = 2\pi \text{ rpm number}/60$ ).

Normally, the electrode current described in equation (2) is measured by a slow-rate potential scan (10 mV/s or 5 mV/s) in order to maintain an electrochemical steady state of electrode and to reduce the charging current to a negligible level.

However, when measuring the powder catalyst coating on an RDE, we found that the large charging current is not negligible because of a high-surface-area electrode. The electrode double-layer charging current [2] can be described as

$$i = \nu C_d + [(E_i/R_s - \nu C_d) \exp(-t/R_s C_d)] . \quad (5)$$

Here,  $\nu$  is the potential scan rate,  $C_d$  is the double-layer capacitance,  $R_s$  is the solution resistance,  $E_i$  is the potential at initial time, and  $t$  is time. If the potential scan rate is zero, equation (5) becomes

$$i = (E_i/R_s) \exp[-t/(R_s C_d)] . \quad (6)$$

The term  $i$  in equation (6) is the charging current for a potential step  $E_i$ . If we wait long enough, the charging current will decay to a negligible level. For our experiment, we used 15 s for the decay time and 1 s for the measurement.

Another problem in using potential scan to measure the reaction current by RDE is the disturbance of adsorption or electrode self-reaction



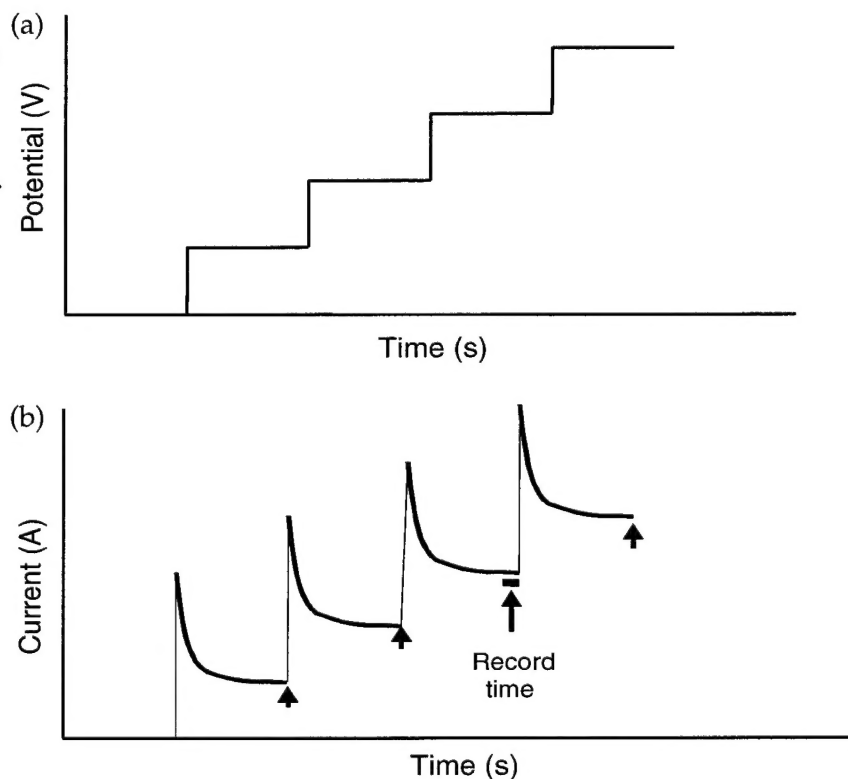
phenomena. The adsorption or electrode self-reaction current [2] can be described as

$$i_p = n^2 F^2 / (4RTvA\Gamma^*) \quad (7)$$

Here,  $i_p$  is the peak current of a reversible adsorption,  $R$  is the gas constant,  $T$  is the absolute temperature, and  $\Gamma^*$  is the electrode surface excess of the species. If the potential scan rate is zero, then the current caused by adsorption and electrode self-reaction will decay to a negligible level.

Here, an RDE method by multiple small potential steps is suggested to measure the reaction current at an RDE to reduce the charging and adsorption current. Figure 1 shows schematic profiles of multiple small potential steps and the resulting current response. For each potential step, only one current value is recorded, and this is at the end of the step. From the multiple small potential steps, we can obtain a collection of current points within the whole range of reaction potentials, i.e., a current-potential curve. The charging current is negligible when the reaction current at each potential scan is recorded. Therefore, in the present study, we define the scan rate obtained by the multiple potential steps at an RDE to be 0 V/s, because the potential is not changing when the current is recorded. Furthermore, the adsorption or electrode self-reaction current will not be recorded, because the scan rate is 0 at the electrode. Therefore, more accurate current-potential curves can be obtained with the use of the method of multiple small potential steps for RDE measurement.

Figure 1. Schematic profiles of (a) multiple small potential steps and (b) resulting current signals at rotating disk electrode.



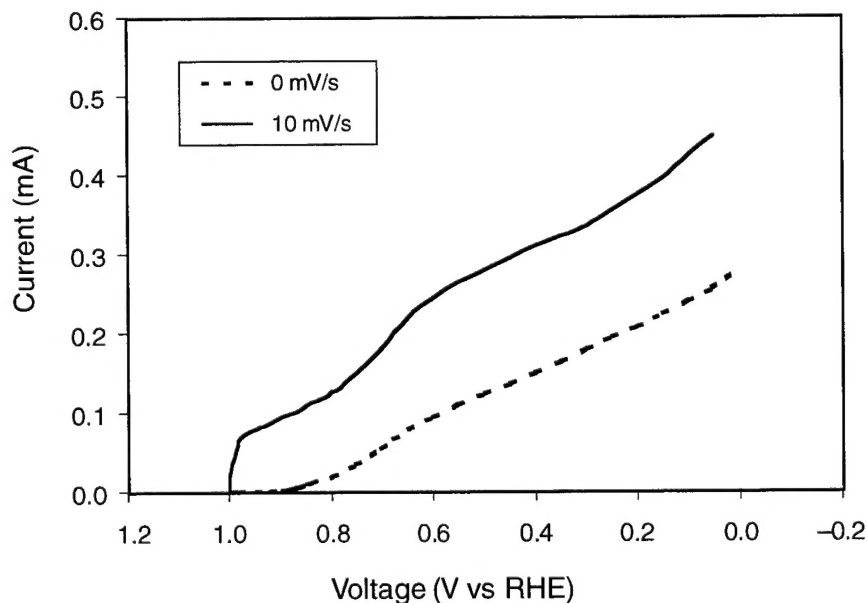
## 4. Results and Discussions

With the RDE method of multiple small potential steps, we can study the electrode kinetics of catalytic reactions at powder-catalyst-coated electrodes. Some specific applications of this method are summarized in this report.

### 4.1 Reduce Charging Current

One of the most important applications of the RDE method of multiple small potential steps is to reduce the charging current at an RDE. Figure 2 shows current-potential curves for oxygen reduction at an HT-FeTPP/PG RDE. After heat treatment, the FeTPP is carbonized and is more conductive and insoluble in any solvent. This means that it can only be coated as a powder of microscopic particle size. The HT-FeTPP-coated electrode has a very high surface area, leading to a large double-layer charging current. The solid curve (10 mV/s) in figure 2, obtained by the classical potential scan RDE method, shows a very large charging current. These data are not reliable for kinetic data analysis. The base current level of the solid line at the initial scan is as large as 70  $\mu$ A. The dashed curve (0 mV/s) was obtained by the RDE method of multiple small potential steps; the double-layer charging current is almost reduced to zero. Once the charging current is eliminated, the current-potential curve for catalytic oxygen reduction at the HT-FeTPP/PG RDE is accurate enough to be used for analysis of the electrode kinetics.

Figure 2. Polarization curves for oxygen reduction at HT-FeTPP-coated RDE in  $O_2$ -saturated 0.5-M  $H_2SO_4$  solution. Catalyst load is 2.0 mg and rotation rate is 100 rpm.



## 4.2 Remove Adsorption or Electrode Self-Reaction Current

Adsorption or electrode self-reaction current should always be avoided when measuring the electrochemical reaction of species in bulk solution. Sometimes the adsorption or electrode self-reaction current is so large, especially at high-surface-area electrodes, that it may cover a whole wave of an electrochemical reaction from bulk solution. Figure 3 shows the current-potential curves of oxygen reduction at a Pd/PG RDE. Since the solid curve (10 mV/s) was obtained from the classical potential scan RDE measurement, we can clearly see a large peak current appearing at 0.8 V, which comes from the surface reaction of the Pd-black catalyst. Because of the large peak current, the RDE data are inaccurate. The dashed curve (0 mV/s) was obtained from the RDE method by multiple small potential steps. The peak current at 0.8 V is completely gone. After the peak current of the electrode self-reaction is removed, the current-potential curve is smoother, and the electrode reaction belongs to the pure reduction of oxygen from bulk solution.

## 4.3 Identify Kinetic Current of Species in Bulk Solution

The electrochemical reaction of species from bulk solution does not always only give diffusion current; it sometimes also gives kinetic current. Furthermore, the current-potential curve caused by the kinetic reaction of the species from bulk solution may show different shapes, or even look like peaks. Because most adsorption or electrode self-reaction waves look like peaks, the identification of adsorption and kinetic currents becomes difficult with the classical potential-scan RDE method.

Figure 4 shows the current-potential curves of methanol oxidation at a Pt/PG RDE in sulfuric acid solution in which the classical potential scan RDE method (10 mV/s) and the multiple potential steps RDE method

**Figure 3.** Polarization curves for oxygen reduction at Pd-black-coated RDE in  $O_2$ -saturated 0.5-M  $H_2SO_4$  solution. Pd-black load is 0.5 mg and rotation rate is 400 rpm.

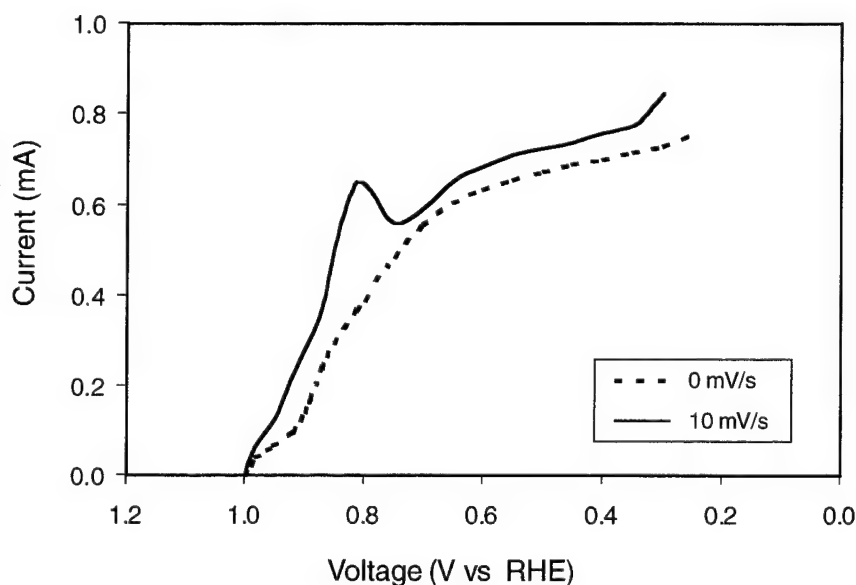
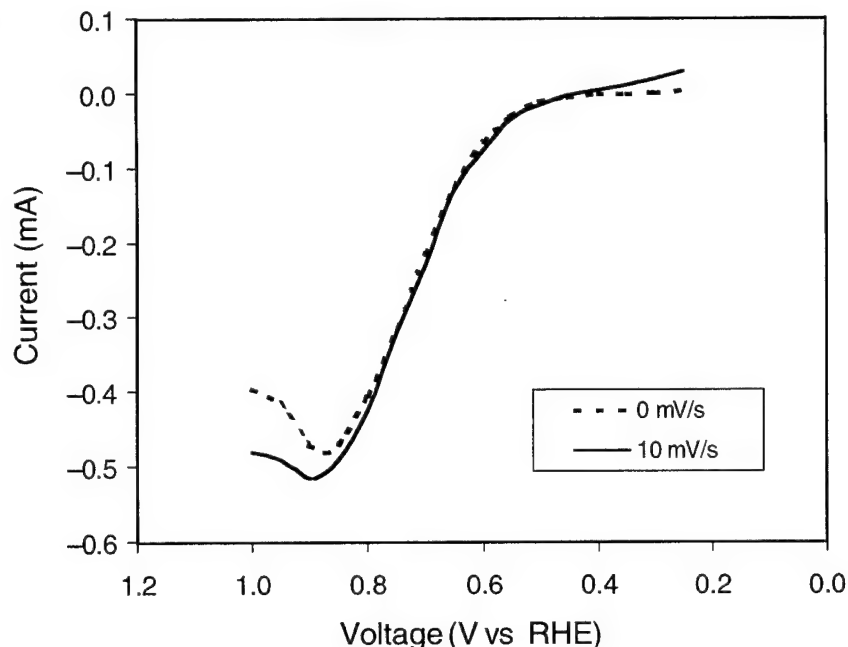


Figure 4. Polarization curves for methanol oxidation at Pt-black-coated RDE in argon-saturated 0.5-M  $\text{H}_2\text{SO}_4$  containing 1.0 M of methanol. Rotation rate is 400 rpm and Pt-black load is 0.5 mg.

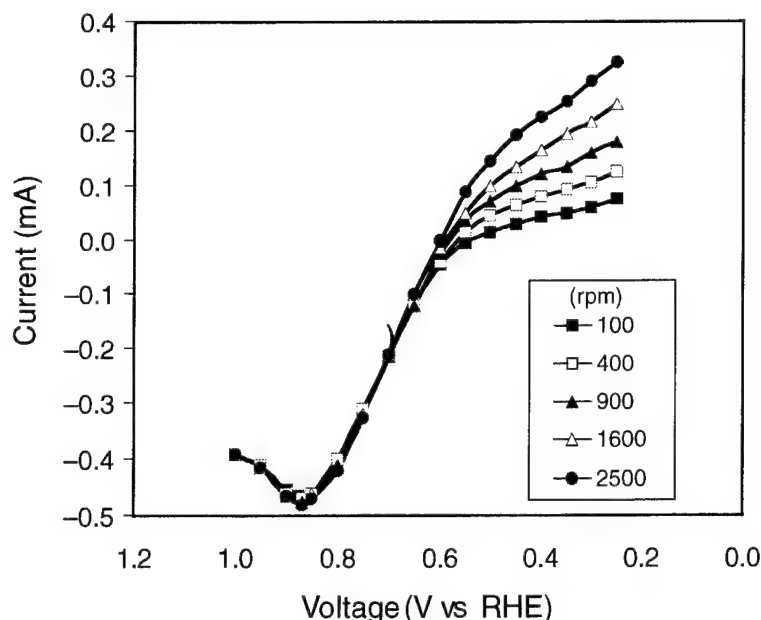


(0 mV/s) have been used. We do not know whether the current is caused by adsorption or by slow electrode reaction. However, with the RDE method of multiple small potential steps, we can easily solve this problem, because at zero scan rate, the adsorption current will be reduced to zero. When the rotation rate was changed from 100 to 2500 rpm, no appreciable current change was observed. Therefore, we can determine that the electrochemical oxidation of methanol in acidic solution at the Pt-black-coated electrode is limited by a slow electrode reaction. For comparison, as previously mentioned, a current-potential curve using classical potential-scan RDE voltammetry (the solid line, 10 mV/s) is shown in figure 4. Because of the influence of charging current, the anodic current for methanol oxidation at 10 mV/s appears larger than that at 0 mV/s, and the background current between 0.4 and 0.2 V increases appreciably.

#### 4.4 Separate Kinetic and Diffusion Reactions

Since the RDE method of multiple small potential steps can be used to identify adsorption and kinetic reactions, it can also be used to separate kinetic and diffusion reactions. Figure 5 shows the current-potential curves of methanol oxidation and oxygen reduction at a Pt/PG RDE in acidic solution. Here, the methanol oxidation is defined as negative current and oxygen reduction as positive current. The methanol oxidation wave is shown in the lower part of the figure, and the oxygen reduction wave is shown in the upper part; they are clearly separated at zero current. Even with an increase in the rotation rate from 100 to 2500 rpm, the wave in the lower part in the figure still does not change; however, the wave at the upper part increases appreciably with the rotation rate. Apparently, the oxygen reduction is identified as a diffusion wave, but methanol oxidation is identified as a kinetic wave.

Figure 5. Polarization curves for oxygen reduction and methanol oxidation at Pt-black-coated RDE in O<sub>2</sub>-saturated 0.5-M H<sub>2</sub>SO<sub>4</sub> containing 1.0 M of methanol. Scan rate is 0 mV/s and Pt-black load is 0.5 mg.



#### 4.5 An Example of Application

One application of the RDE method of multiple small potential steps is to study the catalytic kinetics of oxygen reduction on heat-treated metalloporphyrins. Figure 6 shows a series of current-potential curves for oxygen reduction at an HT-FeTPP/CoTPP/PG RDE in O<sub>2</sub>-saturated 0.5-M sulfuric acid electrolyte. The baseline currents for all curves are near zero, which implies that the double-layer charging currents are negligible. All current-potential curves are smooth, and no adsorption phenomena are observed. With increasing rotation rate, the catalytic current increases. No flat plateaus can be seen at the current-potential curves for all rotation rates, which is most likely because of a low concentration of catalytic sites at the electrode [17].

One can perform the kinetic analysis of oxygen reduction at the powder-catalyst-coated electrode with Koutecky-Levich plot [2] using equation (4). Figure 7 shows the Koutecky-Levich plots obtained from the data in figure 6. As expected, all plots are straight lines. With increasing potential, the intercept becomes larger in the figure, which implies that a kinetic process for catalytic oxygen reduction at the powder-catalyst-coated electrode becomes slower when potential goes up.

For calculating the rate constants of catalytic oxygen reduction, one must use the diffusion coefficient and the concentration of oxygen in bulk solution. The diffusion coefficient of O<sub>2</sub> ( $1.7 \times 10^{-5} \text{ cm}^2 \text{ s}^{-1}$ ) and the concentration of O<sub>2</sub> ( $1.3 \times 10^{-6} \text{ mol/cm}^3$ ) were obtained from the literature [17]. The rate constants for catalytic oxygen reduction at the HT-FeTPP/CoTPP/PG electrode were calculated with the results of the Koutecky-Levich plots in figure 7 and summarized in table 1. With decreasing electrode potential, the rate constant becomes significantly larger.

Figure 6. Polarization curves at various rotation rates for oxygen reduction at HT-FeTPP/CoTPP-coated RDE in  $O_2$ -saturated 0.5-M  $H_2SO_4$  solution. Catalyst load is 2.0 mg and scan rate is 0 mV/s.

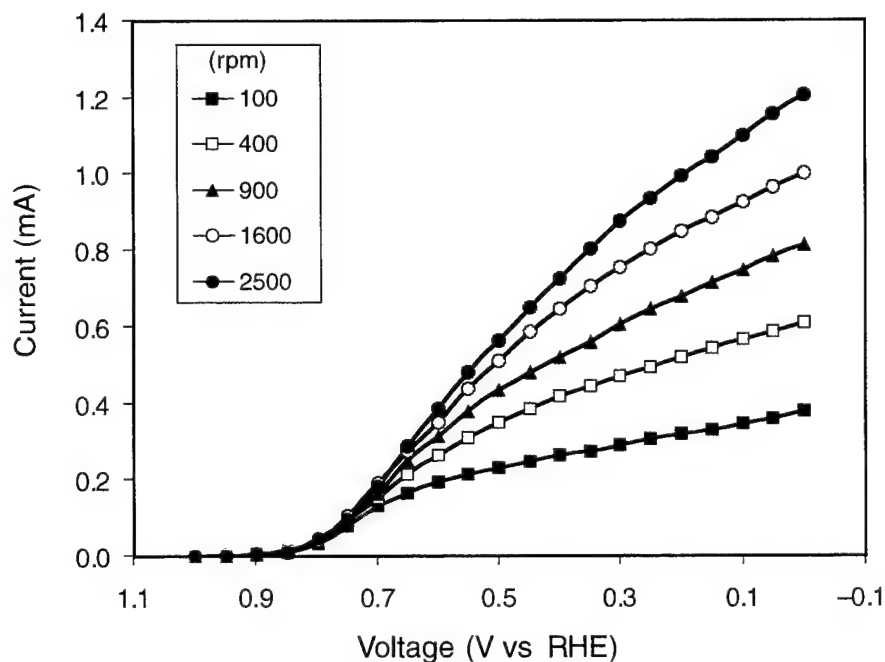


Figure 7. Koutecky-Levich plot for oxygen reduction at HT-FeTPP/CoTPP-coated RDE in  $O_2$ -saturated 0.5-M  $H_2SO_4$  solution. Catalyst load is 2.0 mg. Dashed line represents calculated results for  $O_2$  four-electron reduction by diffusion process.

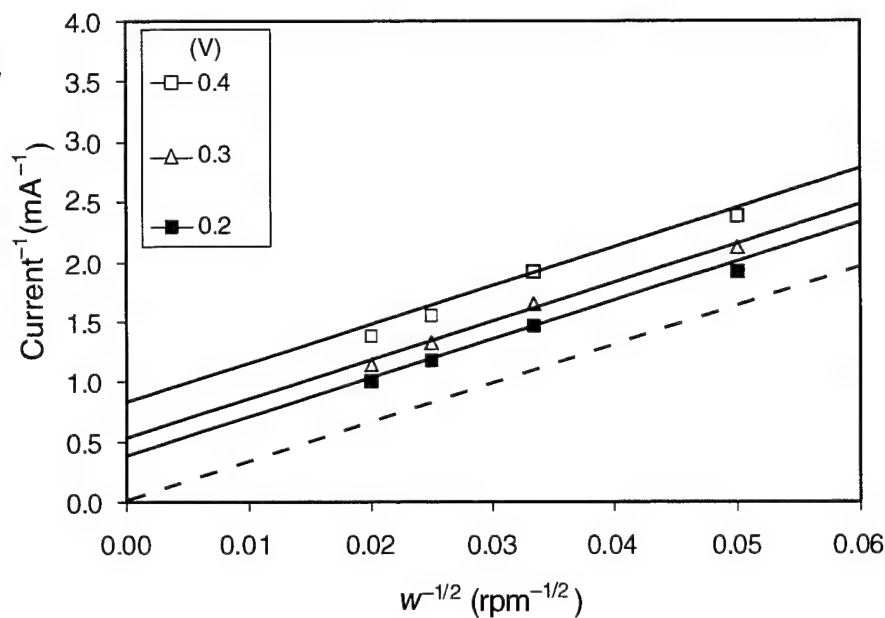


Table 1. Kinetic rate constants for catalytic oxygen reduction at HT-FeTPP-CoTPP/PG electrode in  $O_2$ -saturated 0.5-M  $H_2SO_4$  solution.

Voltage (V)	$K \Gamma_{cat}$ (cm/s)
0.2	0.026
0.3	0.020
0.4	0.014

## 5. Conclusions

An RDE method of multiple small potential steps was used for improving the accuracy of classical potential scan at an RDE. Several benefits of the new RDE method have been summarized, including reducing charging current, removing adsorption current, identifying kinetic current, and separating kinetic and diffusion reactions. With the new RDE method, one can study high-surface-area powder catalysts via the RDE. An example of using this new method was a study of catalytic oxygen reduction at a heat-treated, metalloporphyrin-coated RDE. The kinetic analysis of catalytic oxygen reduction at the powder-catalyst-coated electrode was achieved with the use of the Koutecky-Levich plot.

## Acknowledgments

We wish to thank the U.S. Department of Army and the U.S. Army Materiel Command for their financial support. This project was also supported by the U.S. Army Research Laboratory Director's Research Initiative Program.

## References

1. V. G. Levich, *Physicochemical Hydrodynamics*, Prentice-Hall, Englewood Cliffs, NJ (1962), p 60.
2. A. J. Bard, *Electrochemical Methods, Fundamental and Applications*, John Wiley & Sons, New York (1980), p 283.
3. E. Yeager, "Recent Advances in the Science of Electrocatalysis," *J. Electrochem. Soc.* **128** (1981), C160.
4. C. Shi and F. C. Anson, "(5, 10, 15, 20-Tetramethylporphyrinato)cobalt(II): A Remarkable Active Catalyst for the Electroreduction of  $O_2$  to  $H_2O$ ," *Inorg. Chem.* **37** (1998), p 1037.
5. D. Chu and S. Gilman, "The Influence of Methanol on  $O_2$  Electroreduction at a Rotating Pt Disk Electrode in Acid Electrolyte," *J. Electrochem. Soc.* **141** (1994), p 1770.
6. C. K. Chang, H. Y. Liu, and I. Abdalmuhdi, "Electroreduction of Oxygen By Pillared Cobalt Cofacial Diporphyrin Catalysts," *J. Am. Chem. Soc.* **106** (1984), p 2725.
7. P. A. Forshey and T. Kuwana, "Electrochemistry of Oxygen Reduction 4. Oxygen to Water Conversion by Iron(II) Tetrakis(N-Methyl-4-Pyridyl)Porphyrin via Hydrogen-Peroxide," *Inorg. Chem.* **22** (1983), p 699.
8. R. Jiang and S. Dong, "Rotating Ring Disk Electrode Theory Dealing with Nonstationary Electrocatalysis: Study of the Electrocatalytic Reduction of Dioxygen at Cobalt Protoporphyrin Modified Electrode," *J. Phys. Chem.* **94** (1990), p 7471.
9. R. Jiang and S. Dong, "Application of Linear Rotation-Scan RRDE Theory in Electrochemical Measurement," *Electrochim. Acta* **35** (1990), p 1451.
10. M. S. Wilson and S. Gottesfeld, "Thin-film Catalysis Layers for Polymer Electrolyte Fuel Cell Electrodes," *J. Appl. Electrochem.* **22** (1992), p 1.
11. A. J. Apply and E. B. Yeager, "Polymer Electrolyte Membrane Fuel Cells," *Energy* **11** (1986), p 137.
12. E. A. Ticianelli, C. R. Derouin, and S. Srinivasan, "Localization of Platinum in Low Catalyst Loading Electrodes to Attain High-Power Densities in SPE Fuel-Cells," *J. Electroanal. Chem.* **251** (1988), p 275.
13. J. C. Amphlett, R. M. Baumert, R. F. Mann, B. A. Reppley, and P. R. Roberge, "Performance Modeling of the Ballard-Mark-IV Solid Polymer Electrolyte Fuel-Cell 1. Mechanistic Model Development," *J. Electrochem. Soc.* **142** (1995), p 1.
14. D. Chu and R. Jiang, "Comparative Studies of Polymer Electrolyte Membrane Fuel Cell Stack and Single Cell," *J. Power Sources* **80** (1999), p 226.



15. D. Chu and R. Jiang, "Performance of Polymer Electrolyte Membrane Fuel Cell (PEMFC) Stacks Part I. Evaluation and Simulation of an Air-Breathing PEMFC Stack," *J. Power Sources* **83** (1999), p 128.
16. C. L. Ni and F. C. Anson, "Relation Between the Reduction Potentials of Adsorbed and Unadsorbed Cobalt(III), Tetrakis(N-Methylpyridinium-4-Yl)Porphyrin and Those Where It Catalyzes the Electroreduction of Dioxygen," *Inorg. Chem.* **24** (1985), p 4754.
17. R. Jiang and F. C. Anson, "The Origin of Inclined Plateau Currents in Steady-State Voltammograms for Electrode Processes Involving Electrocatalysis," *J. Electroanal. Chem.* **305** (1991), p 171.

## Distribution

Admnstr  
Defns Techl Info Ctr  
Attn DTIC-OCF  
8725 John J Kingman Rd Ste 0944  
FT Belvoir VA 22060-6218

Ofc of the Secy of Defns  
Attn ODDRE (R&AT)  
The Pentagon  
Washington DC 20301-3080

Ofc of the Secy of Defns  
Attn OUSD(A&T)/ODDR&E(R) R J Trew  
3080 Defense Pentagon  
Washington DC 20301-7100

Advry Grp on Elect Devices  
Attn Documents  
Crystal Sq 4  
1745 Jefferson Davis Hwy Ste 500  
Arlington VA 22202

AMCOM MRDEC  
Attn AMSMI-RD W C McCorkle  
Redstone Arsenal AL 35898-5240

CECOM  
Night Vision/Elect Dir  
Attn AMSEL-RD-NVD  
FT Belvoir VA 22060-5806

Commander  
CECOM R&D  
Attn AMSEL-IM-BM-I-L R Hamlen  
Attn AMSEL-IM-BM-I-L-R Stinfo Ofc  
Attn AMSEL-IM-BM-I-L-R Techl Lib  
FT Monmouth NJ 07703-5703

DARPA  
Attn R Nowak  
3701 N Fairfax Dr  
Arlington VA 22203-1714

Dir for MANPRINT  
Ofc of the Deputy Chief of Staff for Prsnl  
Attn J Hiller  
The Pentagon Rm 2C733  
Washington DC 20301-0300

SMC/CZA  
2435 Vela Way Ste 1613  
El Segundo CA 90245-5500

US Army ARDEC  
Attn AMSTA-AR-TD M Fisette  
Bldg 1  
Picatinny Arsenal NJ 07806-5000

Commander  
US Army CECOM  
Attn AMSEL-RD-CZ-PS-B M Brundage  
FT Monmouth NJ 07703-5000

US Army CECOM  
Rsrch Dev & Engrg Ctr  
Attn AMSEL-RD-AS-BE E Plichta  
FT Monmouth NJ 07703-5703

US Army Info Sys Engrg Cmnd  
Attn AMSEL-IE-TD F Jenia  
FT Huachuca AZ 85613-5300

US Army Natick RDEC  
Acting Techl Dir  
Attn SBCN-T P Brandler  
Natick MA 01760-5002

US Army Simulation, Train, & Instrmntn  
Cmnd  
Attn AMSTI-CG M Macedonia  
Attn J Stahl  
12350 Research Pkwy  
Orlando FL 32826-3726

US Army Soldier & Biol Chem Cmnd  
Dir of Rsrch & Techlgy Dirctr  
Attn SMCCR-RS I G Resnick  
Aberdeen Proving Ground MD 21010-5423

US Army Tank-Automtv Cmnd  
Rsrch, Dev, & Engrg Ctr  
Attn AMSTA-TR J Chapin  
Warren MI 48397-5000

## Distribution (cont'd)

US Army Train & Doctrine Cmnd  
Battle Lab Integration & Techl Dirctr  
Attn ATCD-B  
Attn ATCD-B J A Klevecz  
FT Monroe VA 23651-5850

US Army White Sands Missile Range  
Attn STEWS-IM-ITZ Techl Lib Br  
White Sands Missile Range NM 88002-5501

US Military Academy  
Mathematical Sci Ctr of Excellence  
Attn MDN-A LTC M D Phillips  
Dept of Mathematical Sci Thayer Hall  
West Point NY 10996-1786

Nav Rsrch Lab  
Attn Code 2627  
Washington DC 20375-5000

Nav Surface Warfare Ctr  
Attn Code B07 J Pennella  
17320 Dahlgren Rd Bldg 1470 Rm 1101  
Dahlgren VA 22448-5100

Marine Corps Liaison Ofc  
Attn AMSEL-LN-MC  
FT Monmouth NJ 07703-5033

USAF Rome Lab Tech  
Attn Corridor W Ste 262 RL SUL  
26 Electr Pkwy Bldg 106  
Griffiss AFB NY 13441-4514

AF Wright Aeronautical Labs  
Attn AFWAL-POOS-2 R Marsh  
Wright-Patterson AFB OH 45433

DARPA  
Attn S Welby  
3701 N Fairfax Dr  
Arlington VA 22203-1714

Hicks & Associates Inc  
Attn G Singley III  
1710 Goodrich Dr Ste 1300  
McLean VA 22102

Palisades Inst for Rsrch Svc Inc  
Attn E Carr  
1745 Jefferson Davis Hwy Ste 500  
Arlington VA 22202-3402

Director  
US Army Rsrch Ofc  
Attn AMSRL-RO-D JCI Chang  
Attn AMSRL-RO-EN B Mann  
PO Box 12211  
Research Triangle Park NC 27709-2211

US Army Rsrch Lab  
Attn AMSRL-CI-AI-R Mail & Records Mgmt  
Attn AMSRL-CI-AP Techl Pub (3 copies)  
Attn AMSRL-CI-LL Techl Lib (3 copies)  
Attn AMSRL-DD J M Miller  
Attn AMSRL-RO-PS R Paur  
Attn AMSRL-SE J M McGarrity  
Attn AMSRL-SE J Pellegrino  
Attn AMSRL-SE-D E Scannell  
Attn AMSRL-SE-DC D Chu (25 copies)  
Attn AMSRL-SE-DC R Jiang  
Attn AMSRL-SE-DC C Walker  
Attn AMSRL-SE-DC S Gilman  
Attn AMSRL-SE-E J Mait  
Adelphi MD 20783-1197

REPORT DOCUMENTATION PAGE			Form Approved OMB No. 0704-0188	
Public reporting burden for this collection of information is estimated to average 1 hour per response, including the time for reviewing instructions, searching existing data sources, gathering and maintaining the data needed, and completing and reviewing the collection of information. Send comments regarding this burden estimate or any other aspect of this collection of information, including suggestions for reducing this burden, to Washington Headquarters Services, Directorate for Information Operations and Reports, 1215 Jefferson Davis Highway, Suite 1204, Arlington, VA 22202-4302, and to the Office of Management and Budget, Paperwork Reduction Project (0704-0188), Washington, DC 20503.				
1. AGENCY USE ONLY (Leave blank)		2. REPORT DATE August 2000		3. REPORT TYPE AND DATES COVERED Progress, Oct 1998-Oct 1999
4. TITLE AND SUBTITLE Steady-State Potential Scan at Rotating Disk Electrode and Applications			5. FUNDING NUMBERS DA PR: PE: 62120A	
6. AUTHOR(S) Rongzhong Jiang, Charles Walker, and Deryn Chu				
7. PERFORMING ORGANIZATION NAME(S) AND ADDRESS(ES) U.S. Army Research Laboratory Attn: AMSRL-SE-DC email: rjiang@arl.mil 2800 Powder Mill Road Adelphi, MD 20783-1197			8. PERFORMING ORGANIZATION REPORT NUMBER ARL-TR-2230	
9. SPONSORING/MONITORING AGENCY NAME(S) AND ADDRESS(ES) U.S. Army Research Laboratory 2800 Powder Mill Road Adelphi, MD 20783-1197			10. SPONSORING/MONITORING AGENCY REPORT NUMBER	
11. SUPPLEMENTARY NOTES ARL PR: 9NV4VV AMS code: 622120.H16				
12a. DISTRIBUTION/AVAILABILITY STATEMENT Approved for public release; distribution unlimited.			12b. DISTRIBUTION CODE	
13. ABSTRACT (Maximum 200 words) A method of multiple small potential steps was applied to obtain current-potential curves at a rotating disk electrode (RDE), which is more accurate than the classical potential scan RDE method. Several basic benefits of the new RDE method were summarized, including reducing charging current, removing adsorption current, identifying kinetic current, and separating kinetic and diffusion reactions. The practical application of this new method is to study high-surface-area powder catalysts for fuel cell research. An example of using this new method was demonstrated by measurement of the current-potential curves of catalytic oxygen reduction on a heat-treated, metalloporphyrins-coated graphite RDE. A successful kinetic analysis of catalytic oxygen reduction at the powder-catalyst-coated electrode was achieved.				
14. SUBJECT TERMS RDE, potential step, fuel cell, electrode kinetics, oxygen reduction			15. NUMBER OF PAGES 21	
			16. PRICE CODE	
17. SECURITY CLASSIFICATION OF REPORT Unclassified	18. SECURITY CLASSIFICATION OF THIS PAGE Unclassified	19. SECURITY CLASSIFICATION OF ABSTRACT Unclassified	20. LIMITATION OF ABSTRACT UL	